JOURNAL OF PHYSICAL ORGANIC CHEMISTRY
J. Phys. Org. Chem. 2001; **14:** 432–443
DOI:10.1002/poc.385

Cleft-like hexaamine ligands containing large heteroaromatic moieties as receptors for both anions and metal cations†

Carla Bazzicalupi, Andrea Bencini,* Emanuela Berni, Antonio Bianchi,* Patrizia Fornasari, Claudia Giorgi, Andrea Masotti, Piero Paoletti* and Barbara Valtancoli

Department of Chemistry, University of Florence, Via Maragliano 75/77, I-50144 Florence, Italy

Received 1 December 2000; Revised 26 February 2001; Accepted 6 March 2001

ABSTRACT: Ligands **L1** and **L2** contain two ethylenediamine chains linked to the 2,9 and 6,6′ positions of phenanthroline and bipyridyl, respectively. Their molecular architecture defines a coordinative 'cleft,' a potential binding site for metals and anionic species. Their coordination properties toward Zn(II), Cd(II) and Pb(II) were studied by means of potentiometric, microcalorimetric and UV–vis spectrophotometric measurements. In the $[ML]^{2+}$ complexes (**L** = **L1** or **L2**), the metal is enveloped inside the ligand cleft, as shown by the crystal structure of the $[ZnL2]^{2+}$ cation. On the other hand, the analysis of the thermodynamic data for metal complexation reveals that in the $[ML]^{2+}$ complexes some nitrogen donors are weakly bound, or not bound, to the metal, owing to the presence of a rigid heteroaromatic unit, which leads to a stiffening of the ligands. Both **L1** and **L2**, in their protonated forms, behave as multifunctional receptors for the nucleotide anions at neutral or slightly acidic pH, giving 1:1 complexes. Binding of diphosphate, triphosphate, ATP and ADP was studied by means of potentiometry and ^{1}H and ^{31}P NMR spectroscopy. Charge–charge and hydrogen bonding interactions take place between the polyphosphate chain of nucleotides and the polyammonium groups of **L1** and **L2**, whereas the adenine moiety shows charge–dipole interactions with the ammonium groups and π-stacking with the heteroaromatic units of the receptors. Copyright © 2001 John Wiley & Sons, Ltd.

KEYWORDS: polyamine; proton binding; metal coordination; anion coordination; nucleotides; supramolecular chemistry; molecular recognition

INTRODUCTION

In the last few years there has been considerable interest in the development of new polyamine receptors.[1–22] Open-chain and macrocyclic polyamine ligands, containing appropriate binding sites and/or cavities of suitable size and shape, may be designed to form selective inclusion complexes. Special attention has been devoted to the design and synthesis of polyamine receptors able to coordinate metal ions, with the aim of studying their behavior as selective complexing agents and ionophores.[1–12] Furthermore, even without the involvement of metal cations, polyamine ligands may undergo extensive protonation in aqueous solution, forming highly charged polyammonium cations, able to coordinate anionic species, through charge–charge and hydrogen bond interactions.[13–22] Structural factors have been shown to play significant roles in determining the strength of the interactions between the polyaza receptor and the guest species. Aromatic subunits are often introduced as integral parts of the host molecules. In particular, several macrocycles containing 2,2′-bipyridyl or 1,10-phenanthroline moieties have recently been synthesized.[23–26] These units are rigid and provide two aromatic nitrogens whose unshared electron pairs may act cooperatively in cation binding. At the same time, these heteroaromatic units may offer an optimal binding site for the coordination of nucleotide anions or nucleobases, through π-stacking and hydrophobic interactions.

Recently, we reported the synthesis of a new series of cyclic and acyclic polyamine ligands, such as **L1**, **L2**[25] and **L3**,[26] containing a phenanthroline or a dipyridine unit.

**Correspondence to:* A. Bencini, A. Bianchi or P. Paoletti, Department of Chemistry, University of Florence, Via Maragliano 75/77, I-50144 Florence, Italy.
Email: benc@chim1.unifi.it
†Dedicated to Professor Hans-Jörg Schneider on the occasion of his 65th birthday.
Contract/grant sponsor: Ministero dell'Università e della Ricerca Scientifica e Tecnologica; *Contract/grant number:* COFIN 2000.
Contract/grant sponsor: CNR.

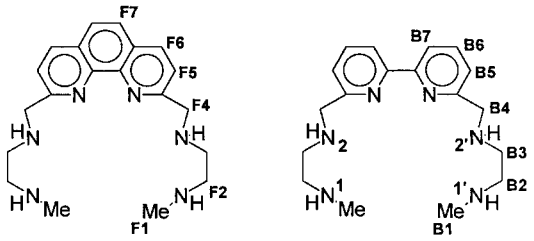

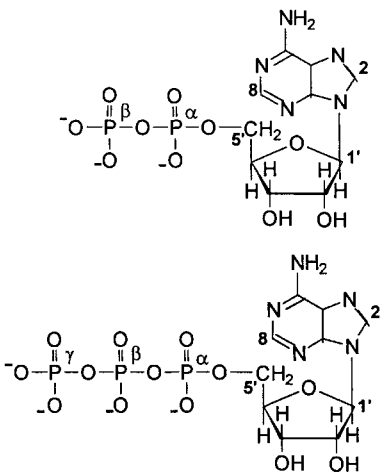

Scheme 1

A previous investigation on the metal coordination properties of phenanthroline-containing macrocycles, such as **L3**, revealed that the phenanthroline unit acts as binding site for metal cations.[26,27] On the other hand, the insertion of this large and rigid heteroaromatic unit within a macrocyclic framework leads to stiffening of the macrocyclic backbone and precludes the simultaneous participation of the heteroaromatic donors and the benzylic amine groups, adjacent to the phenanthroline unit in metal binding.[26,27] At the same time, these macrocycles present, in their protonated species, a molecular organization which allows multipoint binding with anionic forms of nucleotides, through the formation of salt bridges between the ammonium groups and the phosphate chains and π-stacking and hydrophobic interactions between the phenanthroline unit and the adenine moiety of substrates.[20a]

We have now extended this study to the open-chain ligands **L1** and **L2**, which contain two ethylenediamine chains linked to the 2,9 and 6,6′ positions of phenanthroline and dipyridine, respectively. The particular molecular architecture of these two ligands defines a coordinative 'cleft' in which both metal ions and anions can be lodged. In this paper we report on the binding features of these ligands toward metal cations with different size and stereochemical requirements, such as Zn(II), Cd(II) and Pb(II), and toward inorganic phosphate anions and nucleotide anions (ATP and ADP).

RESULTS AND DISCUSSION

Ligand proton transfer properties

Table 1 lists the thermodynamic parameters experimentally determined for the protonation reactions involving **L1** and **L2**. The distribution of the protonated species formed at different pH values by **L2** is illustrated in Fig. 1. The protonation constants and the enthalpic and entropic contributions of **L1** and **L2** are similar for each step of protonation and follow the trend found for the analogous polyamine ligands containing only secondary amine groups, characterized by decreasing protonation constants as the protonation degree, i, increases, and by largely favourable ($\Delta H_i^{\circ} < 0$, $i = 1$–4, Table 1) enthalpic contributions to ligand protonation.[28] In particular the enthalpy changes ($-\Delta H_i^{\circ}$) found in each protonation step are significantly higher than the analogous values reported for protonation of 1,10-phenanthroline and 6,6′-dipyridine ($-\Delta H^{\circ} = 20$ and 17 kJ mol^{-1}, respectively),[29] which can be considered the most appropriate

Table 1. Thermodynamic parameters for **L1** and **L2** protonation 0.1 M, (NMe_4Cl 298.1 K)

	Log K	
	L1	**L2**
$L + H^+ = HL^+$	9.62(1)	9.98(1)
$HL^+ + H^+ = H_2L^{2+}$	9.30(1)	9.48(1)
$H_2L^{2+} + H^+ = H_3L^{3+}$	5.96(1)	6.08(1)
$H_3L^{3+} + H^+ = H_4L^{4+}$	4.63(2)	5.32(1)
	$-\Delta H$ (kJ mol^{-1})	
	L1	**L2**
$L + H^+ = HL^+$	41.38(8)	40.67(5)
$HL^+ + H^+ = H_2L^{2+}$	43.05(7)	42.85(3)
$H_2L^{2+} + H^+ = H_3L^{3+}$	33.44(8)	29.89(5)
$H_3L^{3+} + H^+ = H_4L^{4+}$	38.0(1)	37.28(4)
	$T\Delta S$ (kJ mol^{-1})	
	L1	**L2**
$L + H^+ = HL^+$	13.4(1)	16.3(1)
$HL^+ + H^+ = H_2L^{2+}$	10.0(1)	11.2(1)
$H_2L^{2+} + H^+ = H_3L^{3+}$	0.5(1)	4.8(1)
$H_3L^{3+} + H^+ = H_4L^{4+}$	−11.7(2)	−6.9(1)

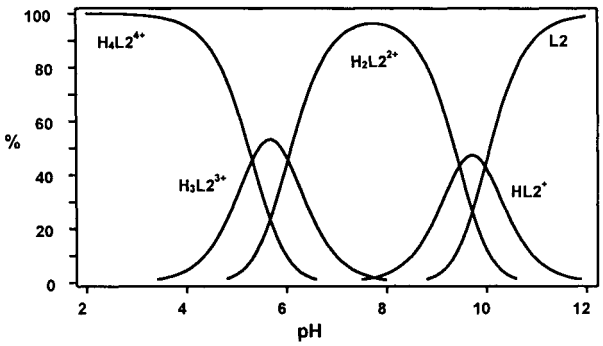

Figure 1. Distribution diagram of the protonated forms of **L2**. 0.1 M NMe_4Cl, 298.1 K

reference compounds for the heteroaromatic moieties of **L1** and **L2**, indicating that such moieties are not directly involved in the protonation processes.

For both **L1** and **L2**, the entropic contributions to each protonation step decrease with increasing degree of protonation, as expected considering the electrostriction effect due to higher solvation of the more protonated receptors.

UV spectra recorded on solutions containing **L1** or **L2** at various pH values do not show significant variations in the pH range 3–11 ($\lambda_{max} = 271$ nm, $\varepsilon = 40\,500$ $dm^3\ mol^{-1}\ cm^{-1}$ and $\lambda_{max} = 290$ nm, $\varepsilon = 12\,400$ $dm^3\ mol^{-1}\ cm^{-1}$, at pH 7, for **L1** and **L2**, respectively) confirming that the aromatic nitrogens are not involved in protonation. In the case of **L2**, however, a slight red shift of the absorption band is observed at strongly acidic pH ($\lambda_{max} = 296$ nm, $\varepsilon = 13\,300$ $dm^3\ mol^{-1}\ cm^{-1}$ at pH 1.5), suggesting that protonation of the dipyridine unit takes place only at strongly acidic pH values. These data suggest that the first four protonation steps of **L1** and **L2** take place on the four aliphatic amine groups.

To obtain further information on the protonation pattern of **L1** and **L2**, we also analyzed the variations with pH of their ^{1}H NMR spectra. Figure 2 reports the ^{1}H NMR chemical shifts of the protons of **L2** as a function of pH. The ^{1}H NMR spectrum of **L2** at pH 12 shows a singlet at 2.10 ppm (integrating six protons and attributed to the hydrogen atoms of the methyl groups, HB1), two triplets at 2.45 and 2.57 (4H each, hydrogen atoms HB2 and HB3, respectively), a singlet at 4.77 (4H, B4), a triplet at 8.13 ppm and two doublets at 7.65 and 8.34 ppm for the aromatic protons HB6, HB5 and HB7. These spectral features indicate a C_{2v} time-averaged symmetry. This symmetry is preserved throughout all the pH range investigated.

In the pH range 11–8, where the first two protons bind to the ligand (Fig. 1), the signal of the hydrogen atoms HB1 and HB2 in the α-position with respect to N1 exhibits a downfield shift, whereas the other signals do not shift appreciably. This suggests that the first two protonation steps involve the terminal nitrogens N1 and N1′. This higher proton affinity of the nitrogen atoms N1 and N1′ in comparison with N2 and N2′ can be ascribed to the inductive effect of the heteroaromatic moiety on the adjacent N2 and N2′ amine groups. In the pH range 7–4 the macrocycle binds two further protons, giving the $[H_4\mathbf{L2}]^{4+}$ species (Fig. 1). The formation of this tetraprotonated form markedly affects the pattern of the ^{1}H NMR spectra. In particular, the signals of HB3 and HB4 bear a remarkable downfield shift (Fig. 2). In contrast, the signals of HB1 and HB2 do not shift appreciably in this pH range. These spectral features indicate that the third and fourth protonation step takes place on the benzylic nitrogens N2 and N2′.

It is interesting that the signals of the aromatic protons HB5–HB7 do not display significant shifts in the pH range 11–3, indicating that the heteroaromatic nitrogens are not involved in proton binding. A slight downfield shift is observed for HB5 and HB7 only below pH 3, probably due to the formation of small amounts of pentaprotonated $[H_5\mathbf{L2}]^{5+}$ species, which is formed at too low pH values to be detected by means of potentiometric measurements. The pH dependence of the ^{1}H NMR spectra of **L1** is almost equal to that found for **L2**, indicating that a similar protonation mechanism occurs in aqueous solution.

Metal binding

Crystal structure of $[ZnL2](ClO_4)_2 \cdot 0.5H_2O$. The molecular structure consists of complexed cations $[Zn\mathbf{L2}]^{2+}$, perchlorate anions and water solvent molecules. The asymmetric unit contains two independent molecules. The ORTEP[30] drawings of the $[Zn\mathbf{L2}]^{2+}$ cations in the two molecules (herein denoted A and B) are shown in Fig. 3(a) and (b), respectively. Table 2 lists selected bond distances and angles for the coordination sphere of

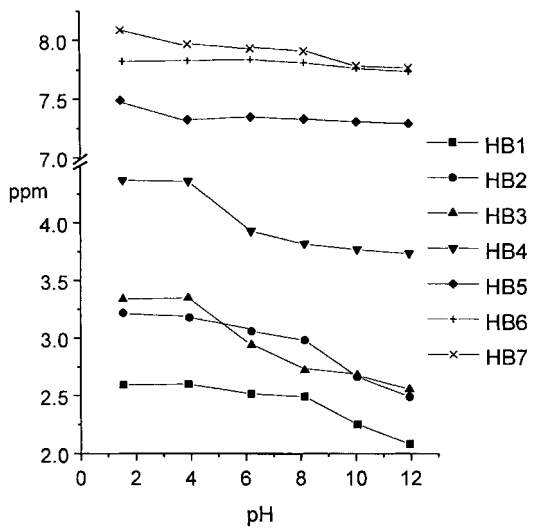

Figure 2. Experimental ^{1}H chemical shifts of **L2** as a function of pH

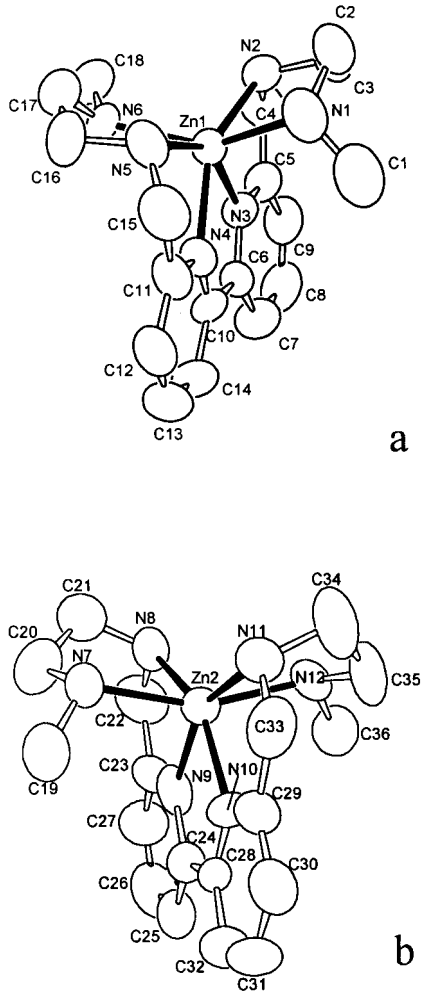

Figure 3. ORTEP drawings of the $[Zn\mathbf{L2}]^{2+}$ cation in the (a) A and (b) B molecules (see text)

Zn(II). The Zn(II) ions in A and B display slightly different coordination geometries, although in both cases the coordination environments can be best described as distorted octahedral.

In complex A the metal is hexacoordinated by the dipyridine nitrogens N3 and N4 and by the amine groups N1, N2, N5 and N6; N2, N3, N4 and N5 define the equatorial plane [maximum deviation = 0.17(1) Å for N5] and N1 and N6 the apical positions of the distorted octahedron. The Zn—N1 and Zn—N6 bonds [Zn—N1 2.120(8) Å; Zn—N6 2.127(8) Å] form angles of 20.1(3)° and 13.0(3)°, respectively, with the normal to the basal plane. The metal ion lies 0.063(2) Å above the basal plane, shifted toward N1. It should be noted that both the benzylic amine groups N2 and N5 are coordinated at longer distances [Zn—N2 2.315(9) Å; Zn—N5 2.362(9) Å] than the other nitrogen donors (Table 2). As already found for other phenanthroline- and dipyridine-containing polyamine ligands,[26,27] the rigidity of the heteroaromatic moiety does not allow the simultaneous optimal coordination of both heteroaromatic and benzylic nitrogen donors to the metal. As a consequence, the benzylic nitrogen atoms are usually not bound[26,27] or, as in the present case, are weakly bound to the metal.

In complex B the basal plane of the octahedron is defined by the N8, N9, N10 and N11 donors [maximum deviation 0.08(1) Å for N9] while N7 and N12 occupy the apical positions. The Zn—N7 and Zn—N12 bonds form angles of 12.7(3)° and 11.7(3)° with the normal to the basal plane. The metal ion lies in this plane. As in the A complex, the two benzylic nitrogens N11 and N8 are coordinated at longer distances [Zn2—N11 2.275(9) Å; Zn2—N8 2.294(9) Å] than the other nitrogen donors (see Table 2).

Considering the ligand conformation, in both A and B complexes the two aromatic rings of the dipyridine moiety are almost coplanar, forming dihedral angles of 6.8(4)° and 7.0(4)° in the A and B complexes, respectively. In both complexes the two aliphatic diamine chains lie on opposite sides with respect to the mean plane defined by the dipyridine unit. The most significant difference between the ligand conformation in the A and B complexes concerns the C—N—C—C and N—C—C—N torsional angles of the two aliphatic side chains. In complex A, the two aliphatic moieties N1—N2 and N5—N6 show different sequences of torsional angles ($g\ g - t\ g$ and $t\ g - t\ g$, respectively), whereas in complex B, both the N7—N8 and N11—N12 chains show the same sequence ($-t\ g\ g - g$).

In both the A and B complexes, however, the resulting screw conformation allows the ligand to 'wrap' around the metal cation, which is, in consequence, enveloped inside the ligand cleft.

Inspection of the crystal packing reveals that the two conformers are associated through a hydrogen bond interaction involving a bridging perchlorate anion. In particular, the O14 oxygen of this anion gives rise to a hydrogen bond with the N5 nitrogen of complex A [N5···O14 3.41(2) Å] and two hydrogen bonds with the N7 and N11 nitrogen atoms of a symmetry-related ($x + 1$, $-y + 1/2$, $z + 1/2$) complex B [N7···O14 3.31(2) Å, N11···O14 3.34(2) Å]. This structural constraint may contribute to the generation of two non-equivalent complexes in the asymmetric unit.

Zn(II), Cd(II) and Pb(II) coordination in aqueous solution. The formation of the Zn(II), Cd(II) and Pb(II) complexes with ligands **L1** and **L2** was investigated by means of potentiometric and microcalorimetric measurements in aqueous solution (0.1 M NMe_4Cl, 298.1 K). The complexes formed and the corresponding thermodynamic parameters are reported in Table 3. The thermodynamic parameters for the metal complexes with the aliphatic hexaamine 1,14-bis(methylamino)-3,6-9,12,-tetrazatetradecane, **L4**,[12b] where an ethylenediamine unit replaces the phenanthroline or dipyridyl units of **L1** and **L2**, are also reported in Table 3 for comparison. The

Table 2. Selected bond lengths (Å) and angles (°) for [Zn**L2**]$(ClO_4)_2 \cdot 0.5H_2O$

A molecule		B molecule	
Zn(1)— N(3)	2.120(8)	Zn(2)— N(10)	2.069(10)
Zn(1)— N(1)	2.125(10)	Zn(2)— N(9)	2.133(9)
Zn(1)— N(6)	2.127(8)	Zn(2)— N(12)	2.150(9)
Zn(1)— N(4)	2.153(9)	Zn(2)— N(7)	2.154(9)
Zn(1)— N(2)	2.315(9)	Zn(2)— N(11)	2.275(9)
Zn(1)— N(5)	2.362(9)	Zn(2)— N(8)	2.294(9)
N(3)— Zn(1)— N(1)	108.3(4)	N(10)— Zn(2)— N(9)	75.0(4)
N(3)— Zn(1)— N(6)	100.0(3)	N(10)— Zn(2)— N(12)	97.5(4)
N(1)— Zn(1)— N(6)	147.8(4)	N(9)— Zn(2)— N(12)	99.5(4)
N(3)— Zn(1)— N(4)	74.1(3)	N(10)— Zn(2)— N(7)	100.4(3)
N(1)— Zn(1)— N(4)	100.6(4)	N(9)— Zn(2)— N(7)	97.7(4)
N(6)— Zn(1)— N(4)	101.5(3)	N(12)— Zn(2)— N(7)	157.8(4)
N(3)— Zn(1)— N(2)	74.2(4)	N(10)— Zn(2)— N(11)	77.0(4)
N(1)— Zn(1)— N(2)	78.1(4)	N(9)— Zn(2)— N(11)	151.7(4)
N(6)— Zn(1)— N(2)	95.8(3)	N(12)— Zn(2)— N(11)	80.4(4)
N(4)— Zn(1)— N(2)	145.9(4)	N(7)— Zn(2)— N(11)	91.0(4)
N(3)— Zn(1)— N(5)	145.3(4)	N(10)— Zn(2)— N(8)	150.0(4)
N(1)— Zn(1)— N(5)	86.6(4)	N(9)— Zn(2)— N(8)	75.3(4)
N(6)— Zn(1)— N(5)	78.3(3)	N(12)— Zn(2)— N(8)	91.6(4)
N(4)— Zn(1)— N(5)	72.4(4)	N(7)— Zn(2)— N(8)	79.2(3)
N(2)— Zn(1)— N(5)	140.5(4)	N(11)— Zn(2)— N(8)	132.9(4)

distribution diagrams of the **L1** complexes are reported in Fig. 4. These data allow one to infer some general trends.

(i) Ligands **L1** and **L2** show a similar good ability to coordinate Zn(II), Cd(II) and Pb(II) and the complexes are formed in aqueous solution even at acidic pH values (Fig. 4).
(ii) The $[ML]^{2+}$ complexes (**L** = **L1** and **L2**) are easily protonated at neutral or acidic pH values, forming, in the case of Cd(II) and Pb(II), up to tri- or tetraprotonated species.
(iii) The Zn(II) and Cd(II) complexes show a similar thermodynamic stability, much higher than that of the Pb(II) complexes. This trend is generally observed with polyamine ligands.[29]

Both **L1** and **L2** are strong metal binders in aqueous solution. The stability of their complexes is noticeably higher than that reported for the corresponding complexes with **L4**.[12b,c] This observation indicates that the insertion of the heteroaromatic binding unit within the ligand backbone leads to an enhancement of complex stability.

In order to obtain further information on the role played by the phenanthroline and bipyridyl units in metal coordination, the reaction of complex formation was followed by means of UV spectra recorded on aqueous solutions containing ligand **L1** or **L2** (3×10^{-4} M) and Zn(II), Cd(II) and Pb(II) in various molar ratios at pH 7. In the case of **L1** the phenanthroline moiety gives a family sharp band at 271 nm ($\varepsilon = 37\,100$ $dm^3\,mol^{-1}\,cm^{-1}$). Solutions containing **L1** and increasing amounts of metals, up to a 1:1 molar ratio, show a marked decrease of the adsorbance. A linear correlation between the metal to ligand ratio and the ε values is found up to a 1:1 molar ratio (under these conditions, $\lambda_{max} = 269$ nm, $\varepsilon = 33\ 600$ $dm^3\,mol^{-1}\,cm^{-1}$). As reported for Zn(II) binding to 2,2′ -dipyridine alone, Zn(II) complexation by **L2** gives a marked red shift of the absorption band. Significant shifts of the UV band are also observed for Cd(II) and Pb(II) complexes with this ligand. A summary of the spectral features of the metal complexes with **L1** and **L2** are reported in Table 4. The UV data in Table 5 account for the involvement of the phenanthroline and bipyridyl moieties in metal binding in the $[ML]^{2+}$ complexes in aqueous solution. This suggestion is further confirmed by the crystal structures of the [Zn**L2**]$(ClO_4)_2$ complex, which shows that both the aromatic nitrogens are bound to the metal.

The higher stability of the complexes with phenanthroline- and dipyridyl-containing ligands with respect to the **L4** ligands can be ascribed, in principle, to the different molecular topology of the ligands and/or to the different binding ability of aliphatic secondary amine groups with respect to heteroaromatic groups. On the other hand, the analysis of the thermodynamic parameters in Table 3 shows that the higher stability of the **L1** and **L2** complexes than the **L4** complexes is mainly due to the entropic contributions, at least in the case of Zn(II) and Cd(II) complexation, whereas the enthalpic contributions to the formation of the **L1** and **L2** complexes are less favorable compared with those found for the **L4** complexes.[12b]

The comparison of the enthalpic terms for the formation of the $[ML1]^{2+}$ and $[ML2]^{2+}$ complexes with those of the $[ML4]^{2+}$ complexes suggests a lower overall interaction of **L1** and **L2** with metal ions with respect to **L4**, for which it was suggested that five or six nitrogen donors are involved in metal coordination.[12b] Indeed, both **L1** and **L2**

Table 3. Thermodynamic parameters for Zn(II), Cd(II) and Pb(II) complexation with **L1, L2** and **L4** (0.1 M NMe_4Cl, 298.1 K)

Reaction	Log K	$-\Delta G°$ (kJ mol^{-1})	$-\Delta H°$ (kJ mol^{-1})	$T\Delta S°$ (kJ mol^{-1})
$Zn^{2+} + \mathbf{L1} = Zn\mathbf{L1}^{2+}$	16.17(2)	91.9(1)	44.3(1)	47.6
$Zn\mathbf{L1}^{2+} + H^+ = Zn\mathbf{L1}H^{3+}$	8.86(3)	50.5(1)	40.9(1)	9.6
$Zn^{2+} + \mathbf{L2} = Zn\mathbf{L2}^{2+}$	16.52(3)	94.1(1)	46.5(1)	47.6
$Zn\mathbf{L2}^{2+} + H^+ = Zn\mathbf{L2}H^{3+}$	4.35(4)	24.8(1)	21.3(1)	3.5
$Zn^{2+} + \mathbf{L4} = Zn\mathbf{L4}^{2+}$	14.02[a]	79.8	49.3	30.5
$Zn\mathbf{L4}^{2+} + H^+ = Zn\mathbf{L4}H^{3+}$	3.93			
$Cd^{2+} + \mathbf{L1} = Cd\mathbf{L1}^{2+}$	16.03(2)	91.4(1)	59.0(1)	32.4
$Cd\mathbf{L1}^{2+} + H^+ = Cd\mathbf{L1}H^{3+}$	5.19(2)	29.6(1)	35.1(1)	−5.5
$Cd\mathbf{L1}H^{3+} + H^+ = Cd\mathbf{L1}H_2{}^{4+}$	4.67(5)	26.6(1)	27.6(1)	−1.0
$Cd\mathbf{L1}H_2{}^{4+} + H^+ = Cd\mathbf{L1}H_3{}^{5+}$	3.43(5)	19.6(1)	30.1(1)	−10.5
$Cd^{2+} + \mathbf{L2} = Cd\mathbf{L2}^{2+}$	16.31(2)[a]	93.0(1)	47.5(6)	45.5
$Cd\mathbf{L2}^{2+} + H^+ = Cd\mathbf{L2}H^{3+}$	4.92(4)	28.0(1)	30.1(1)	−2.1
$Cd\mathbf{L2}H^{3+} + H^+ = Cd\mathbf{L2}H_2{}^{4+}$	4.88(2)	27.8(1)	32.7(1)	−4.9
$Cd\mathbf{L2}H_2{}^{4+} + H^+ = Cd\mathbf{L2}H_3{}^{5+}$	3.73(7)	21.2(1)	20.8(1)	0.4
$Cd^{2+} + \mathbf{L4} = Cd\mathbf{L4}^{2+}$	15.29	86.9	64.8	22.1
$Cd\mathbf{L4}^{2+} + H^+ = Cd\mathbf{L4}H^{3+}$	5.83			
$Pb^{2+} + \mathbf{L1} = Pb\mathbf{L1}^{2+}$	12.78(5)	72.7(3)	47.2(1)	25.5
$Pb\mathbf{L1}^{2+} + H^+ = Pb\mathbf{L1}H^{3+}$	8.22(5)	46.8(3)	44.3(1)	2.5
$Pb\mathbf{L1}H^{3+} + H^+ = Pb\mathbf{L1}H_2{}^{4+}$	5.26(4)	30.1(3)	30.9(1)	−0.8
$Pb\mathbf{L1}H_2{}^{4+} + 2H^+ = Pb\mathbf{L1}H_4{}^{6+}$	6.29(5)	35.9(3)	13.0(1)	22.9
$Pb^{2+} + \mathbf{L2} = Pb\mathbf{L2}^{2+}$	11.28(4)	64.4(3)	43.9(1)	20.5
$Pb\mathbf{L2}^{2+} + H^+ = Pb\mathbf{L2}H^{3+}$	8.49(2)	48.4(1)	43.0(1)	5.4
$Pb\mathbf{L2}H^{3+} + H^+ = Pb\mathbf{L2}H_2{}^{4+}$	5.67(1)	32.2(1)	33.9(1)	−1.7
$Pb^{2+} + \mathbf{L4} = Pb\mathbf{L4}^{2+}$	9.97[b]			
$Pb\mathbf{L4}^{2+} + H^+ = Pb\mathbf{L4}H^{3+}$	9.29			
$Pb\mathbf{L4}H^{3+} + H^+ = Pb\mathbf{L4}H_2{}^{4+}$	6.72			

[a] From Ref. 12b.
[b] From Ref. 12c.

show a fairly high tendency to give protonated complexes and, as shown in Fig. 4 for the $[M\mathbf{L1}]^{2+}$ complexes, protonated species are formed in large amounts at slightly acidic pH. Most likely, water molecules occupy the free binding sites at the metal in these protonated species. The enthalpy contributions for the first protonation step of the $[M\mathbf{L}]^{2+}$ complexes are very high (Table 3), in some cases similar to those found for protonation of the free amines. These observations strongly suggest that in both the $[M\mathbf{L1}]^{2+}$ and $[M\mathbf{L2}]^{2+}$ complexes some amine groups are not bound, or are only weakly bound, to the metal. Most likely, the rigidity of the heteroaromatic units does not allow the simultaneous binding of all six donors, as previously observed in metal complexes with phenanthroline-containing polyazamacrocycles.[26,27] Actually, the crystal structure of the $[Zn\mathbf{L2}]^{2+}$ cation shows that the two benzylic nitrogens [N2 and N5 in Fig. 3(a)] are only weakly involved in metal coordination, interacting with the metal at longer distances (ca 2.3 Å) than the other nitrogen donors (2.0–2.1 Å).

As anticipated above, the stabilization of the **L1** and **L2** complexes with respect the **L4** complexes is mainly due to a more favorable entropic contribution. Two main factors can be invoked to rationalize this aspect: (i) **L1** and **L2** present a preformed cavity where the metals can be lodged, with a consequent lower entropic cost for the process of ligand rearrangement upon metal complexation. (ii) Complexes with primary or secondary amines are normally more solvated than complexes with tertiary or heteroaromatic amines, owing to the inability of the latter to give N—H···OH_2 hydrogen bonds. This may result in a larger desolvation of ligands **L1** and **L2** upon metal complexation, leading to a more favorable entropic contribution with respect to **L4**.

Phosphate anion binding in aqueous solution

Protonation of the receptors gives charged species which may enable **L1** and **L2** to form stable complexes with anionic species in aqueous solution. Binding of ATP, ADP, diphosphate and triphosphate by **L1** and **L2** was studied by means of potentiometric measurements and, in the case of ATP and ADP, by ^1H and ^{31}P NMR measurements.

The formation of anionic complexes with polyammonium receptors is strictly pH dependent and, therefore, the solution equilibria can be studied by pH-metric titrations. Table 5 gives the cumulative and stepwise equilibrium constants for the species formed by **L1** and **L2**. The stability constants of the **L1** complexes with diphosphate are too low to be determined confidently by means of potentiometric measurements. Although in some cases the formation of both 1:1 and 2:1 anion–macrocycle complexes has been observed,[31] the data analysis with the program HYPERQUAD[32] under our

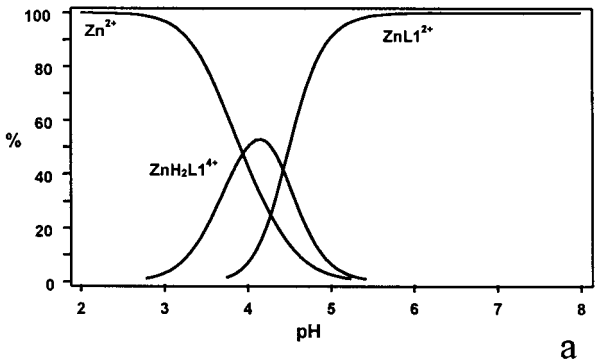

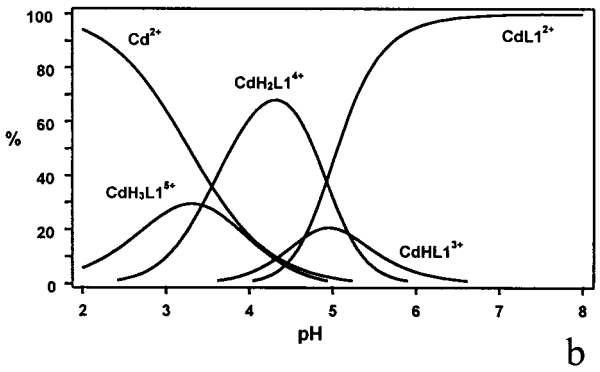

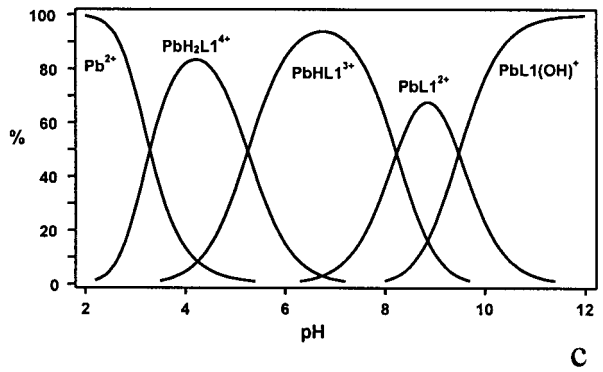

Figure 4. Distribution diagrams for the systems (a) Zn–**L1**, (b) Cd–**L1** and (c) Pb–**L1**. [**L1**] = [M] = 1×10^{-3} mol dm^{-3} (M = Zn, Cd or Pb), 0.1 M NMe_4Cl, 298.1 K

experimental conditions revealed 1:1 stoichiometries for all the species detected.

By examining the different values of the stability constants, several main features can be readily noticed. For a given ligand the strength of the interaction generally increases with increase in the degree of ligand protonation. For instance, the stability constants for the interaction of ATP^{4-} with **L1** and **L2** vary, respectively, from log $K = 4.08$ and 4.46 for the diprotonated macrocycles to log $K = 4.26$ and 5.45 for the macrocycles in their tetraprotonated forms. An increasing number of protonated polyammonium functions increases the receptor ability to give charge–charge and hydrogen bonding interactions with the anionic substrates. High degrees of protonation of the complexes imply protonation of nucleotides and, therefore, a low negative charge of the substrates. As a consequence, no interaction between protonated macrocycles and the uncharged H_3ADP and H_4ATP or monocharged H_2ADP^- and H_3ATP^- substrates was found by potentiometry. The formation of the substrate–polyammonium receptor adducts, therefore, takes place mainly from weakly alkaline to slightly acidic pHs, as shown in Fig. 5, which displays the distribution diagrams for the ADP–**L2** and ATP–**L2** systems. For the system ATP–**L2**, the percentage of overall complexed species is almost 90% in the pH range 4.5–7, whereas for the system ADP–**L2** it is more than 40% in the pH range 4.0–6.5. In both cases, the overall percentages of substrate–receptor complexes decrease at more strongly alkaline or acidic pH. For instance, the percentage of the ATP–**L2** adduct becomes almost negligible at pH 2 and above pH 10.

Comparison of Fig. 5(a) and (b) also indicates a lower interaction of ADP with **L2** with respect to ATP. As can be seen from Table 5, for the same degree of protonation, the ADP complexes with **L1** and **L2** show a lower stability in comparison with the ATP adducts. This behavior can be reasonably ascribed to weaker charge–charge interactions in the ADP complexes, due to lower negative charge on the ADP anion.

Finally, Table 5 indicates that the two receptors show a similar binding ability toward ATP and ADP, as expected considering the similar molecular architecture of the two ligands and the similar charge distribution in their protonated forms. The slightly higher stability of the **L2** adducts may be ascribed to the somewhat higher flexibility of this ligand, which could allow better charge matching between the ammonium function of the protonated receptor and the anionic phosphate chains of nucleotides.

Anion complexation was also followed by recording ^{31}P NMR spectra on solutions containing receptors and substrates in a 1:1 molar ratio at different pH values. Figure 6 shows the ^{31}P chemical shifts of the phosphate groups of ATP in the presence of **L1** (1:1 molar ratio)

Table 4. UV/vis data of ligands **L1** and **L2** and their Zn(II), Cd(II) and Pb(II) complexes

Parameter	**L1**	**L2**
λ (nm) [ε(dm^3 mol^{-1} cm^{-1})]	271 [37 000]	290 [12 400]
	$[ZnL1]^{2+}$	$[ZnL2]^{2+}$
λ (nm) [ε(dm^3 mol^{-1} cm^{-1})]	269 [31 600]	312 [13 300]
	$[CdL1]^{2+}$	$[CdL2]^{2+}$
λ (nm) [ε(dm^3 mol^{-1} cm^{-1})]	271 [30 200]	305 [13 200]
	$[PbL1]^{2+}$	$[PbL2]^{2+}$
λ (nm) [ε(dm^3 mol^{-1} cm^{-1})]	268 [27 700]	308 [13 100]

Table 5. Stability constants (log *K*)[a] of the ADP, ATP, diphosphate and triphosphate adducts with **L1** and **L2**, determined by means of potentiometric measurements in 0.1 mol dm^{-3} NMe_4Cl at 298.1 K

Reaction	**L1**	**L2**	Reaction	**L1**	**L2**
$A = ADP^{3-}$			$A = ATP^{4-}$		
$L + 2H^+ + A^{3-} = H_2LA^-$	21.55(7)		$L + 2H^+ + A^{4-} = H_2LA^{2-}$	23.15(5)	24.65(8)
$L + 3H^+ + A^{3-} = H_3LA$	28.95(3)	29.4(1)	$L + 3H^+ + A^{4-} = H_3LA^-$	30.18(8)	31.00(8)
$L + 4H^+ + A^{3-} = H_4LA^+$	34.96(3)	35.3(1)	$L + 4H^+ + A^{4-} = H_4LA$	36.78(4)	37.71(7)
$L + 5H^+ + A^{3-} = H_5LA^{2+}$	39.71(2)	40.5(1)	$L + 5H^+ + A^{4-} = H_5LA^+$	41.70(3)	43.49(5)
$H_2L^{2+} + A^{3-} = H_2LA^-$	2.63(7)		$H_2L^{2+} + A^{4-} = H_2LA^{2-}$	4.22(5)	5.19(8)
$H_2L^{2+} + HA^{2-} = H_3LA$	3.44(4)	3.1(1)	$H_2L^{2+} + HA^{3-} = H_3LA^-$	4.08(8)	4.46(8)
$H_3L^{3+} + HA^{2-} = H_4LA^+$	3.48(3)	3.2(1)	$H_3L^{3+} + HA^{3-} = H_4LA$	4.71(4)	4.99(7)
$H_4L^{4+} + HA^{2-} = H_5LA^{2+}$	3.61(2)	3.4(1)	$H_4L^{4+} + HA^{3-} = H_5LA^+$	5.01(3)	5.45(5)
Reaction	**L2**		Reaction	**L1**	**L2**
$A = P_2O_7^{4-}$			$A = P_3O_{10}^{5-}$		
$L + 4H^+ + A^{4-} = H_4LA$	37.13(8)		$L + 3H^+ + A^{5-} = H_3LA^{2-}$	29.93(3)	
			$L + 4H^+ + A^{5-} = H_4LA^-$	37.40(2)	37.47(5)
			$L + 5H^+ + A^{5-} = H_5LA$	42.37(2)	43.32(5)
			$L + 6H^+ + A^{5-} = H_6LA^+$	47.06(2)	
$H_2L^{2+} + H_2A^{2-} = H_4LA$	2.62(8)		$H_2L^{2+} + HA^{4-} = H_3LA^{2-}$	2.51(3)	
			$H_3L^{3+} + HA^{4-} = H_4LA^-$	4.02(2)	3.93(5)
			$H_3L^{3+} + H_2A^{3-} = H_5LA$	3.19(2)	3.47(5)
			$H_4L^{4+} + H_2A^{3-} = H_6LA^+$	3.25(2)	

[a] Values in parentheses are standard deviations on the last significant figure.

at different pH values, together with those of free ATP, and Table 6 reports the complexation-induced ^{31}P chemical shifts (CIS) for the nucleotides–**L1** or and–**L2** systems.

The data in Fig. 6 and Table 6 indicate that complexation of substrates produces significant variations in the ^{31}P chemical shifts, as already observed for analogous complexes with other polyammonium macrocyclic receptors.[18,19] Considering ADP complexation, the resonances of both the phosphate groups shift downfield in the presence of the macrocycles. In the case of the ATP complexes with **L1** and **L2**, only the signals of two phosphate groups, P_β and P_γ, show a clear downfield shift upon complexation, while the chemical shift of P_α is almost not influenced by the interaction with the receptors. These observations seem to indicate that in both ATP and ADP the polyammonium functions of the receptors mainly interact with two contiguous phosphate groups of nucleotides. Furthermore, the higher CIS values observed for P_β and P_γ in the ADP and ATP complexes, respectively, suggest a stronger interaction of the terminal phosphate groups with the polyammonium functions of the receptors. At the same time, in the case of ATP, P_α would give an almost negligible interaction. As shown in Fig. 6 for the system ATP–**L1**, the variations of the chemical shifts are strongly pH dependent, being greater in the pH range 4–8 and much lower above pH 9. A similar behavior is also observed for **L2**. This result is in agreement with the potentiometric study of these systems, which has shown that large amounts of the 1:1 receptor–substrate adducts are formed from slight alkaline to acidic pHs, i.e. in the pH region where highly protonated species of the receptors and anionic species of ADP or ATP are simultaneously present in solution. It should also be noted that the CIS values for the **L2** complexes are higher than those for the **L1** adducts, suggesting, once again, a slightly stronger electrostatic interaction between the phosphate groups of nucleotides and the two polyammonium chains of **L2**.

Both the potentiometric and ^{31}P NMR data confirm the important role played by electrostatic force and hydrogen bonding in this kind of interaction. Both ligands contain two diamine chains separated by a rigid spacer. As discussed above, protonation takes place on the aliphatic amine groups. Therefore, it can be proposed that a spatial charge matching between the two protonated polyamine chains and two adjacent phosphate groups of nucleotides gives the major contribution to the complex stability, allowing the formation of multiple electrostatic and hydrogen bond interactions.

On the other hand, comparing the binding of nucleotides and inorganic phosphate anions ($P_2O_7^{4-}$ and $P_3O_{10}^{5-}$), the data in Table 5 show that, for the same negative charge on the anions, triphosphate gives weaker interaction with **L1** and **L2** than ATP, which contains a triphosphate chain similar to that of $P_3O_{10}^{5-}$ (e.g. the addition constants of the triply charged $H_2P_3O_{10}^{3-}$ to $H_3\mathbf{L1}^{3+}$ and $H_4\mathbf{L1}^{4+}$ are 3.19 and 3.25 log units, whereas the addition constants of $HATP^{3-}$ to $H_3\mathbf{L1}^{3+}$ and $H_4\mathbf{L1}^{4+}$ are 4.71 and 5.01 log units). Similarly, the stability of the diphosphate adducts is lower than that of the ADP adducts. In addition to electrostatic interactions

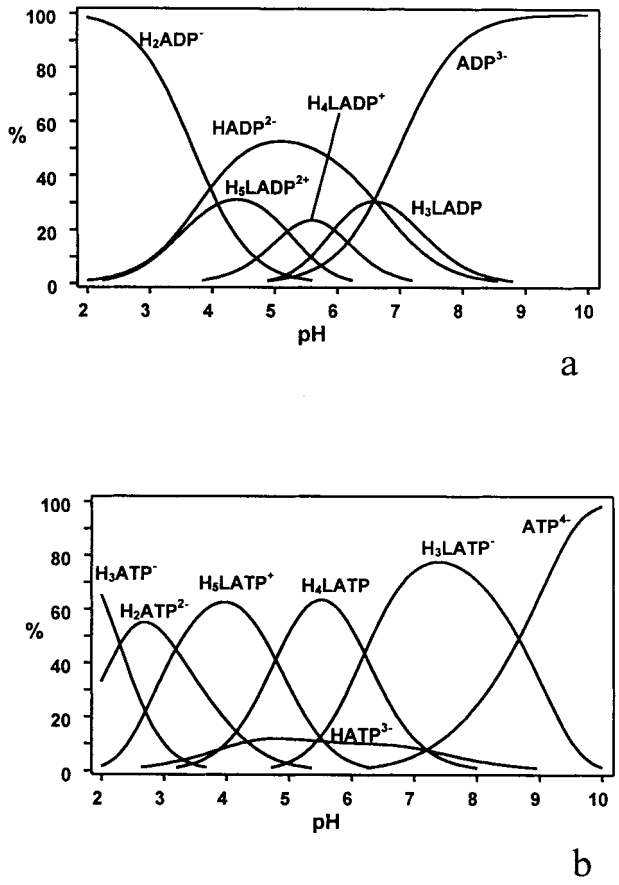

Figure 5. Distribution diagrams for the systems (a) **L2**–ADP (0.1 mol dm^{-3} NMe_4Cl, 298.1 K, [**L2**] = [ADP] = 1×10^{-3} mol dm^{-3}) and (b) **L2**–ATP (0.1 mol dm^{-3} NMe_4Cl, 298.1 K, [**L2**] = [ATP] = 1×10^{-3} mol dm^{-3})

between the phosphate chain and the polyammonium macrocycles, other effects (hydrogen bond interactions between adenine nitrogens and/or hydroxyl groups of nucleotides and polyammonium functions, hydrophobic and/or π-stacking interactions between the heteroaromatic moieties and cation–π system interactions between the charged ammonium group and adenine) may contribute to the complex stability.

The ^{1}H NMR spectra of these systems provide unambiguous evidence for the participation of π-stacking interactions in the stabilization of the adduct species with **L1** and **L2** (for labeling, see Scheme 1). For both ligands, throughout the pH ranges in which interaction occurs, significant upfield displacements are observed for the resonances of the adenine protons H2 and H8 and for the anomeric proton H1′ of the nucleotides and also for the signals of phenanthroline (HF5, HF6 and HF7) or dipyridine (HB5, HB6 and HB7). Minor shifts are observed for the benzylic protons F4 or B4 and for the other protons of the aliphatic chains (<0.2 ppm). Figure 7 shows the ^{1}H chemical shifts for the phenanthroline hydrogens of **L1** in absence and in presence of ATP [Fig. 7(a)] and for the hydrogens H2, H8 and H1′ of ATP [Figure 7(b)] in absence and in presence of **L1** (1:1 molar

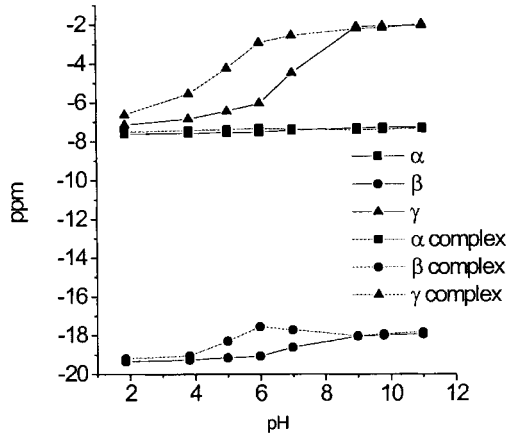

Figure 6. Experimental ^{31}P chemical shifts of free ATP (solid lines) and of ATP in the presence of **L1** (dotted lines) as a function of pH. [**L1**] = [ATP] = 5×10^{-3} mol dm^{-3}, 298.1 K

ratio). As previously observed for the ^{31}P resonances of the phosphate chains, the ^{1}H NMR displacements are strongly pH dependent, being larger at neutral or slightly acidic pHs, where the largest extent of complexation occurs. It is interesting that, once again, these differences are substantially reduced at strongly acidic or alkaline pH, where the interaction vanishes. Table 7 reports the complexation-induced ^{1}H chemical shifts (CIS) for the interaction of **L1** and **L2** with ADP and ATP. It should be noted that the CIS values for ATP and ADP complexation are very high, in particular in the case of **L1** (more than 1 ppm for adenosine protons of ADP or ATP complexed by **L1**), if compared with the CIS values found for ATP or ADP complexation by other polyammonium macrocycles containing phenylene spacers.[19] This can be

Table 6. ^{31}P NMR shifts (δ, ppm) for the **L1** and **L2** adducts with ATP and ADP and complexation-induced ^{1}H NMR chemical shifts (CIS, ppm) for selected protons, measured in D_2O solution at pH 5 (systems ATP–**L1** and ADP–**L1**) and 5.5 (systems ATP–**L2** and ADP–**L2**), 298 K

	L1		**L2**	
ADP	P_α	P_β	P_α	P_β
δ (ppm)	−6.90[a]	−4.52	−6.77	−3.93
CIS	1.02[b]	3.31	1.15	3.91

	L1			**L2**		
ATP	P_α	P_β	P_γ	P_α	P_β	P_γ
δ (ppm)	−7.40	−18.31	−4.24	−7.46	−17.86	−3.62
CIS	0.24	1.27	3.30	0.20	1.72	3.90

[a] From measurements in D_2O solution at pH 5 (systems ATP–**L1** and ADP–**L1**) and 5.5 (systems ATP–**L2** and ADP–**L2**), 298.1 K, with a receptor:substrate molar ratio of 1:1. Under these conditions the degrees of complexation are 55% (ADP–**L1**), 78% (ATP–**L1**), 53% (ADP–**L2**) and 90% (ATP–**L2**).
[b] CIS (for 100% complexation) calculated based on equilibrium constants from Table 5.

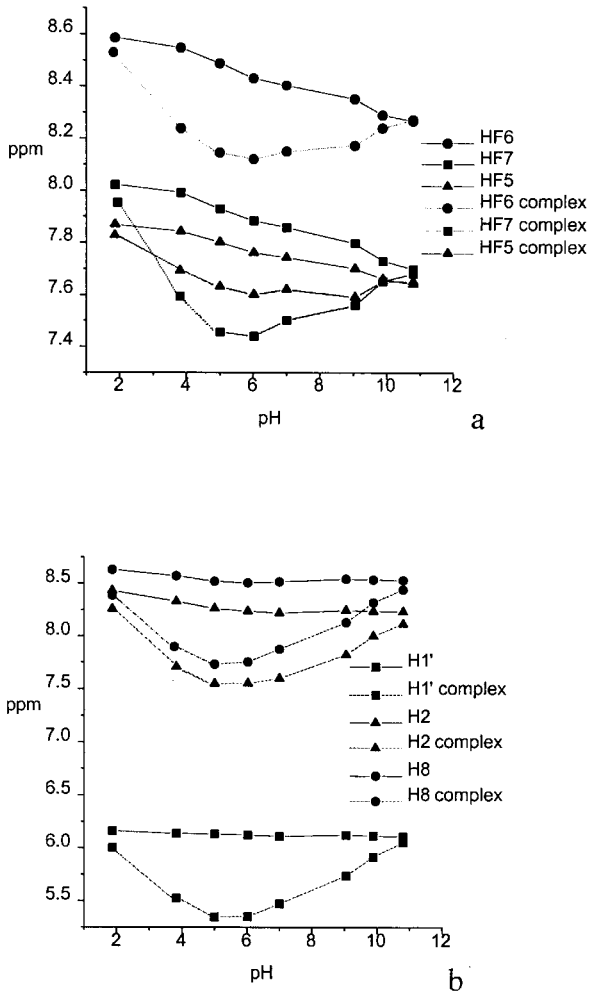

Figure 7. (a) Experimental ^{1}H chemical shifts for the aromatic protons of free **L1** (solid lines) and of **L1** in the presence of ATP (dotted lines). (b) Experimental ^{1}H chemical shifts for the H2, H8 and H1′ protons of free ATP (solid lines) and of ATP in the presence of **L1** (dotted lines). In all experiments **L1** and ATP were in a 1:1 molar ratio (both 5×10^{-3} mol dm^{-3}), 298.1 K

attributed to the insertion in the macrocyclic framework of a large heteroaromatic system, such as phenanthroline, which can give strong π-stacking interactions with the adenine moiety of nucleotides. Lower CIS values are found for the **L2** complexes, probably owing to the less extended aromatic system of dipyridine with respect to phenanthroline.

High CIS values, however, may also be indicative of inclusion, or partial inclusion, of the substrate inside the ligand cleft, as already observed in the case of other polyammonium receptors.[14c,19] Partial inclusion may allow for the simultaneous involvement of electrostatic and π-stacking interactions in the stabilization of the adducts and, additionally, adenine nitrogens and/or hydroxyl groups of the ribose subunits could be properly disposed to give hydrogen bonds with the polyammonium groups of the receptor.

EXPERIMENTAL

General procedures. Ligands **L1** and **L2** were obtained as described previously.[25] Crystals of [Zn**L2**](ClO$_4$)$_2$·0.5H$_2$O were obtained by slow evaporation of an aqueous solution (pH 7) containing Zn(ClO$_4$)$_2$·6H$_2$O and **L2** in an equimolecular ratio. The 300.07 MHz ^{1}H and 75.46 MHz ^{13}C NMR spectra in D$_2$O solutions at different pH values were recorded at 298.1 K in a Varian Unity 300 MHz spectrometer. In the ^{1}H NMR spectra peak positions are reported relative to HOD at 4.75 ppm. Dioxane was used as a reference standard in the ^{13}C NMR spectra ($\delta = 67.4$ ppm). ^{1}H–^{1}H and ^{1}H–^{13}C 2D correlation experiments were performed to assign the signals. Small amounts of 0.01 mol dm^{-3} NaOD or DCl solutions were added to a solution of **L1**·4HBr or **L2**·4HBr to adjust the pD. The pH was calculated from the measured pD values using the following relationship:[33]

$$\mathrm{pH} = \mathrm{pD} - 0.40$$

The ^{31}P NMR spectra were recorded at 81.01 MHz with a Bruker AC-200 spectrometer. Chemical shifts are relative to 85% H$_3$PO$_4$ as external reference. UV–vis spectra were recorded on a Shimadzu UV-2101PC spectrophotometer.

X-ray structural analysis. Crystal data. $C_{36}H_{58}Cl_4N_{12}O_{17}Zn_2$, $M = 1203.48$, monoclinic, $a = 14.714(5)$ Å, $b = 21.220(10)$ Å, $c = 16.47(2)$ Å, $\beta = 99.87(5)°$, volume = 5066(7) Å^3 (by least-squares refinement on diffractometer angles for 25 automatically centered reflections, $\lambda = 0.7107$ Å), space group $P2_1/c$, $Z = 4$, calculated density 1.578 g cm^{-3}, $F(000) = 2488$. Colorless prismatic crystal of approximate dimensions $0.25 \times 0.15 \times 0.1$ mm, $\mu = 1.237$ mm^{-1}, $T = 25$ °C.

Data collection and structure analysis. Analysis on a single crystal of [Zn**L2**](ClO$_4$)$_2$·0.5H$_2$O was carried out with an Enraf-Nonius CAD4 x-ray diffractometer that uses an equatorial geometry; $\theta - 2\theta$ scan with θ scan width = 0.9 + 0.35tan θ, θ scan speed variable, graphite monochromated Mo Kα radiation, 5588 reflections measured ($5° \leq 2\theta \leq 40°$). Intensity data were corrected for Lorentz and polarization effects and an absorption correction was applied once the structure had been solved by the Walker and Stuart method.[34]

The structure was solved by direct methods of SIR92.[35] Anisotropic displacement parameters were used with all the non-hydrogen atoms. All the hydrogen atoms were introduced in calculated positions and their coordinates refined in agreement with the linked atoms, with overall refined temperature factors.

The final agreement factors for 644 refined parameters were $R1 = 0.0616$ [for 2788 reflections with $I > 2\Sigma(I)$] and $wR2 = 0.1868$ (all data). Refinement was performed

Table 7. ^{1}H NMR shifts (δ, ppm) for the **L1** and **L2** adducts with ATP and ADP and complexation-induced ^{1}H NMR chemical shifts (CIS, ppm) for selected protons, measured in D_2O solution at pH 5 (systems ATP–**L1** and ADP–**L1**) and 5.5 (systems ATP–**L2** and ADP–**L2**), 298 K

		HF5	HF6	HF7	H8	H2	H1′
L1	δ	7.63	8.14	7.46			
ATP	δ				7.73	7.55	5.35
	CIS	−0.26	−0.51	−0.71	−1.18	−1.06	−1.17
L1	δ	7.70	8.28	7.63			
ADP	δ				7.81	7.69	5.42
	CIS	−0.16	−0.35	−0.52	−1.13	−0.90	−1.12
		HB5	HB6	HB7	H8	H2	H1′
L2	δ	8.01	7.42	7.78			
ATP	δ				8.24	7.75	5.62
	CIS	−0.18	−0.23	−0.61	−0.68	−0.85	−0.90
L2	δ[a]	8.04	7.37	8.07			
ADP	δ				8.14	7.81	5.70
	CIS	−0.15	−0.28	−0.32	−0.80	−0.78	−0.84

[a] From measurements in D_2O solution at pH 5 (ATP–**L1** and ADP–**L1**) and 5.5 (ATP–**L2** and ADP–**L2**), 298.1 K, with a receptor:substrate molar ratio of 1:1. Under these conditions the complexation degrees are 55% (ADP–**L1**), 78% (ATP–**L1**), 53% (ADP–**L2**) and 90% (ATP–**L2**).
[b] CIS (for 100% complexation) calculated based on equilibrium constants from Table 5.

by means of the SHELXL-93 program.[36] The function minimized was $\Sigma w(F_o^2 - F_c^2)^2$ with $w = 1/[\sigma^2(F_o^2) + (aP)^2 + bP]$and $P = (F_o^2 + 2F_c^2)/3$, where a and b are adjustable parameters.

Potentiometric measurements. Equilibrium constants for protonation and complexation reactions with **L1** and **L2** were determined by pH-metric measurements ($pH = -\log [H^+]$) in 0.1 mol dm^{-3} NMe_4Cl at 298.1 ± 0.1 K, by using the potentiometric equipment and method described previously.[12,37] The combined glass electrode was calibrated as a hydrogen concentration probe by titrating known amounts of HCl with CO_2-free NaOH solutions and determining the equivalence point by Gran's method,[38] which allows one to determine the standard potential $E°$ and the ionic product of water [$pK_w = 13.83(1)$ at 298.1 K in 0.1 mol dm^{-3} NMe_4Cl]. In the metal complexation study 1×10^{-3}–2×10^{-3} mol dm^{-3} ligands and metal ion concentrations were employed, and in the anion coordination study the ligand:anion molar ratio was varied from 0.5 to 5. Protonation constants of phosphate anions were taken from Ref. 20. At least three titration experiments were performed (about 100 data points each) in the pH range 2.5–10.5. The computer program HYPERQUAD[32] was used to calculate equilibrium constants from e.m.f. data. All titrations were treated either as single sets or as separate entities, for each system, without significant variation in the values of the determined constants.

Microcalorimetric measurements. The enthalpies of ligand protonation and metal complexation were determined in 0.1 M NMe_4Cl aqueous solutions at 298.1 K by means of the apparatus described previously.[20b] Protonation enthalpies were determined by addition of NMe_4OH (0.1 M, addition volumes 0.015 cm^3) to an acidic solution of the ligand (5×10^{-3} M, 1.2 cm^3). The complexation enthalpies were determined by means of titration with NMe_4OH (0.1 M, addition volumes 0.015 cm^3) of acidic solutions, containing ligand and M(II) (M = Zn, Cd, Pb). Metal and ligand concentrations were ca 5×10^{-3} mol dm^{-3}. The ionic medium was NMe_4Cl (0.1 M). Under the reaction conditions and employing the protonation and/or stability constants determined at 298.1 K, the concentrations of the species present in solution before and after addition were calculated and the corresponding enthalpies of reaction were determined from the calorimetric data by means of the AAAL program.[39] At least three titrations were performed for each system. The titration curves for each system were treated either as a single set or as separate entities without significant variation in the values of the enthalpy changes.

Acknowledgements

Financial support by the Italian Ministero dell'Università e della Ricerca Scientifica e Tecnologica, within the program COFIN 2000, and by the Italian Research Council (CNR) is gratefully acknowledged.

REFERENCES

1. Bradshaw JS. *Aza-crown Macrocycles*. Wiley: New York, 1993.
2. Izatt RM, Pawlak K, Bradshaw JS. *Chem. Rev.* 1995; **95**: 2529–2586.
3. Gokel GW. *Crown Ethers and Cryptands*. Royal Society of Chemistry: Cambridge, 1991.
4. Lehn JM. *Supramolecular Chemistry*. VCH: New York, 1995.

5. Lu Q, Reibenspies JJ, Martell AE, Motekaitis RJ. *Inorg. Chem.* 1996; **35**: 2630–2636, and references cited therein.
6. Lindoy LF. *The Chemistry of Macrocyclic Ligand Complexes*. Cambridge University Press: Cambridge, 1989.
7. Lindoy LF. *Pure Appl. Chem.* 1997; **69**: 2179–2184.
8. Amendola V, Fabbrizzi L, Mangano C, Pallavicini P, Perotti A, Taglietti A. *J. Chem. Soc. Dalton Trans.* 2000; 185–189.
9. Kaden TA, Tschudin D, Studer M, Brunner U. *Pure Appl. Chem.* 1989; **61**: 879–884.
10. Blake AJ, Champness NR, Hubberstey P, Li WS, Schröder M, Withersby MA. *Coord. Chem. Rev.* 1999; **183**: 117–138.
11. Nelson J, McKee V, Morgan G. *Prog. Inorg. Chem.* 1998; **47**: 167–316.
12. (a) Bazzicalupi C, Bencini A, Berni E, Fedi V, Fusi V, Giorgi C, Paoletti P, Valtancoli B. *Inorg. Chem.* 1999; **38**: 4115–4122; (b) Aragò J, Bencini A, Bianchi A, Garcia-España E, Micheloni M, Paoletti P, Ramirez JA, Rodriguez A. *J. Chem. Soc. Dalton Trans.* 1991; 3077–3083; (c) Andres A, Bencini A, Carachalios A, Bianchi A, Dapporto P, Garcia-España E, Paoletti P, Paoli P. *J. Chem. Soc. Dalton Trans.* 1993; 3507–3513.
13. Izatt RM, Pawlak K, Bradshaw JS, Bruenig RL. *Chem. Rev.* 1991; **91**: 1721–2085.
14. (a) Schneider H-J. *Angew. Chem.* 1991; **30**: 1417–1436; (b) Schneider H-J, Schiestel T, Zimmermann P. *J. Am. Chem. Soc.* 1992; **114**: 7698; (c) Schneider H-J, Blatter T, Palm B, Pfingstag U, Rüdiger V, Theis I. *J. Am. Chem. Soc.* 1992; **114**: 7704–7709; (d) Eliseev AV, Schneider H-J. *J. Am. Chem. Soc.* 1994; **116**: 6081–6088, and references therein.
15. Menger FM, Catlin KK. *Angew. Chem. Int. Ed. Engl.* 1995; **34**: 2147–2149.
16. Reetz MT, Niemeyer CM, Harms K. *Angew. Chem. Int. Ed. Engl.* 1991; **30**: 1472–1474.
17. Bianchi A, Garcia-España E, Bowman-James K. (eds). *Supramolecular Chemistry of Anions*. Wiley-VCH: New York, 1997.
18. (a) Hosseini MW, Lehn JM, Maggiora L, Mertes MP, Mertes KB. *J. Am. Chem. Soc.* 1987; **109**: 537–544; (b) Hosseini MW, Blaker AJ, Lehn JM. *J. Am. Chem. Soc.* 1990; **112**: 3896–3904.
19. Aguilar JA, Garcia-España E, Guerrero JA, Luis SV, Llinares JM, Miravet MF, Ramirez JA, Soriano C. *J. Chem. Soc. Chem. Commun.* 1995; 2237–2238.
20. (a) Bazzicalupi C, Beconcini A, Bencini A, Fusi V, Giorgi C, Masotti A, Valtancoli B. *J. Chem. Soc. Perkin Trans. 2* 1999; 1675–1682; (b) Bazzicalupi C, Bencini A, Bianchi A, Cecchi M, Escuder B, Fusi V, Garcia-España E, Giorgi C, Luis SV, Maccagni G, Marcelino V, Paoletti P, Valtancoli B. *J. Am. Chem. Soc.* 1999; **121**: 6807–6815.
21. (a) Mertes MP, Mertes KB. *Acc. Chem. Res.* 1990; **23**: 413–421; (b) Mason S, Clifford T, Seib L, Kuzcera K, Bowman-James K. *J. Am. Chem. Soc.* 1998; **120**: 8899–8900.
22. Kràl V, Furuta H, Shreder K, Lynch V, Sessler JL. *J. Am. Chem. Soc.* 1996; **118**: 1595–1607.
23. (a) Rodriguez-Ubis J-C, Alpha B, Plancherel D, Lehn JM. *Helv. Chim. Acta* 1984; **67**: 2264–2269; (b) Alpha B, Lehn JM, Mathis G. *Angew. Chem. Int. Ed. Engl.* 1987; **26**: 266–267; (c) Alpha B, Anklam E, Deschenaux R, Lehn JM, Pietraskiewicz M. *Helv. Chim. Acta* 1988; **71**: 1042–1049; (d) Cesario M, Guilhem J, Pascard E, Anklam E, Lehn JM, Pietraskiewicz M. *Helv. Chim. Acta* 1991; **74**: 1157–1162; (e) Lehn JM, Regnouf de Vains JB. *Helv. Chim. Acta* 1992; **75**: 1221–1236; (f) Azéma J, Galaup C, Picard C, Tisnès P, Ramos O, Juanes O, Rodrìguez-Ubis JC, Brunet E. *Tetrahedron* 2000; **56**: 2673–2681, and references cited therein; (h) Newkome GR, Pappalardo S, Gupta VK, Fronczek F. *J. Org. Chem.* 1983; **48**: 4848–4854, and references cited therein.
24. Vidal P-L, Divisia-Blohorn B, Bidan G, Kern J-M, Sauvage J-P, Hazemann J-L. *Inorg Chem.* 1999; **38**: 4203–4210; (b) Weck M, Mohr B, Sauvage J-P, Grubbs RH. *J. Org. Chem.* 1999; **64**: 5463–5471; (c) Rapenne G, Dietrich-Buchecker C, Sauvage J-P. *J. Am. Chem. Soc.* 1999; **121**: 994–1001; (d) Meyer M, Albrecht-Gary A-M, Dietrich-Buchecker CO, Sauvage J-P. *Inorg. Chem.* 1999; **38**: 2279–2287.
25. Bazzicalupi C, Bencini A, Ciattini S, Giorgi C, Masotti A, Paoletti P, Valtancoli B, Navon N, Meyerstein D. *J. Chem. Soc. Dalton Trans.* 2000; 2383–2391.
26. (a) Bazzicalupi C, Bencini A, Fusi V, Giorgi C, Paoletti P, Valtancoli B. *Inorg. Chem.* 1998; **37**: 941–948; (b) Bazzicalupi C, Bencini A, Fusi V, Giorgi C, Paoletti P, Valtancoli B. *J. Chem. Soc. Dalton Trans.* 1999; 393–399; (c) Bencini A, Bianchi A, Fusi V, Giorgi C, Masotti A, Paoletti P. *J. Org. Chem.* 2000; **65**: 7686–7689.
27. (a) Bazzicalupi C, Bencini A, Bianchi A, Fusi V, Giorgi C, Paoletti P, Valtancoli B, Pina F, Bernardo MA. *Inorg. Chem.* 1999; **37**: 3806–3813; (b) Bazzicalupi C, Bencini A, Bianchi A, Fusi V, Giorgi C, Valtancoli B, Pina F, Bernardo MA. *Eur. J. Inorg. Chem.* 1999; 1911–1918.
28. Bencini A, Bianchi A, Garcia España E, Micheloni M, Ramirez JA. *Coord. Chem. Rev.* 1999; **188**: 97–156.
29. Smith RM, Martell AE. *NIST Critical Stability Constants Database, Version 2*. National Institute of Standards and Technology: Gaithersburg, MD, 1995.
30. Johnson CK, Burnett MN. ORTEP-3. Windows version 1.01 by L. Farrugia, *J. Appl. Cryst.* 1997; **30**: 565.
31. Dietrich B, Hosseini MW, Lehn J-M, Session RB. *J. Am. Chem. Soc.* 1981; **103**: 1282.
32. Gans P, Sabatini A, Vacca A. *Talanta* 1996; **43**: 807–812.
33. Covington AK, Paabo M, Robinson RA, Bates RG. *Anal. Chem.* 1968; **40**: 700–706.
34. Walker N, Stuart DD. *Acta Crystallogr. Sect A* 1983; **39**: 158–166.
35. Altomare A, Cascarano G, Giacovazzo C, Guagliardi A. *J. Appl. Crystallogr.* 1993; **26**: 343.
36. Sheldrick GM. SHELXL-93. University of Göttingen: Göttingen, 1993.
37. Bianchi A, Bologni L, Dapporto P, Micheloni M, Paoletti P. *Inorg. Chem.* 1984; **23**: 1201–1205.
38. Gran G. *Analyst (London)* 1952; **77**: 661–671.
39. Vacca A. AAAL Program. Department of Chemistry, University of Florence: Florence, 1997.